

Transverse z -mode waves in the terrestrial electron foreshock

S. D. Bale

Space Sciences Laboratory, University of California, Berkeley

P. J. Kellogg, K. Goetz, and S. J. Monson

School of Physics and Astronomy, University of Minnesota, Minneapolis

Abstract. We examine the phase relation between two orthogonal electric field components for several hundred waveform measurements of intense electron plasma waves in the terrestrial electron foreshock. In general, the phase shift at the carrier frequency is not zero or π as would be expected if the waves were purely electrostatic Langmuir waves, but is a function of the angle between the antennas and the interplanetary magnetic field (IMF). When the antennas are field aligned, the phase shift between the components is large; this value recedes smoothly to zero as the antenna is rotated away from the IMF direction. When solar wind density fluctuations are considered, this is consistent with the dispersion of the electromagnetic z -mode and we assert that the electron foreshock is populated by transverse z -mode waves, not purely longitudinal Langmuir waves. This has implications for conversion to freely propagating modes and large-amplitude saturation mechanisms.

Introduction

The electron foreshock, upstream from the Earth's bow shock, is characterized by a flux of suprathermal electrons away from the shock. Since these particles convection with the solar wind, a velocity selection effect leaves an effective beam near the boundary between the foreshock and solar wind [Filbert and Kellogg, 1979]. This unstable particle distribution is a source of intense electrostatic and electromagnetic wave activity and the operative instabilities and saturation mechanisms are an active research topic.

Historically, plasma wave receivers have been of the swept frequency design, sampling power or amplitude on one or two antennas but without measuring the relative phase. Using the sweep receiver and two orthogonal dipoles on IMP 6, Filbert and Kellogg [1979] established that the electric field vector of the electron plasma waves in the foreshock is usually, but not always, aligned with the IMF direction.

In this letter, we show that the polarization of these waves is not purely longitudinal. Using simultaneously sampled waveforms from two orthogonal antennas, we calculate the phase shift between the two components of the measured carrier wave. While purely longitudinal Langmuir waves would have phase shift of 0 or π , we find that the phase varies with antenna orientation relative to the IMF. Since the solar wind is weakly magnetized ($\Omega_{ce}/\omega_{pe} \lesssim 0.01$), the

relevant large- k magnetized mode is the z - mode (slow extraordinary branch). At large k , z -mode waves are virtually identical to Langmuir waves. However, in the presence of small density fluctuations the z -mode can evolve to small k , where it has a significant transverse component [Krauss-Varban, 1989].

Analysis

Data are used from the Time Domain Sampler (TDS) instrument [Bougeret et al., 1995] on the Wind spacecraft as it made several passes through the terrestrial electron foreshock between April 19 and April 23, 1996 and June 13 and June 15, 1997. The fast channel of the TDS instrument samples 2 orthogonal electric field antennas simultaneously at very high sampling rates; for the data herein, the instrument was configured to sample at 120,000 samples/second on the spacecraft X and Y antennas simultaneously, which have tip-to-tip lengths of 100 m and 15 m respectively. The TDS returns events of 2048 samples, which have been buffered and sorted on the spacecraft to telemeter the largest amplitude events preferentially. A hardware threshold of roughly 0.05 mV/m and the selection algorithm bias this dataset of 895 events to large amplitudes. We calculate the angle ϕ between the X antenna and the IMF vector projected on the spin plane, using 3 second (spin period) resolution magnetic field data from the MFI instrument.

Figure 1 shows the ratio E_x/E_y of RMS electric field on the X and Y antennas as a function of antenna azimuth ϕ ; the theoretical electrostatic response for the antenna system is overplotted assuming a field vector with $k \approx 2\pi/400 \text{ m}^{-1}$, aligned with the IMF. For large k , the ratio of responses does not depend strongly on k . It can be seen that the electric fields are ordered by the magnetic field direction, as previously observed [Filbert and Kellogg, 1979]. Note that for $\phi = 0$ or 180° , we are approximately measuring $E_\parallel/E_\perp = E_x/E_y$, which lies in the range 1 to 10; therefore E_\perp/E_\parallel is approximately 0.1 to 1.

To extract phase information, we apply a cross spectral analysis to the electric field events. The normalized cross spectrum is defined as

$$\tilde{C}(\omega) = \frac{\langle \tilde{S}_x(\omega)\tilde{S}_y^*(\omega) \rangle}{\sqrt{\langle \tilde{S}_x(\omega)\tilde{S}_x^*(\omega) \rangle \langle \tilde{S}_y(\omega)\tilde{S}_y^*(\omega) \rangle}} \quad (1)$$

where \tilde{S} is the Fourier transform of the input signal and the brackets denote ensemble averaging. We use ensembles of 256 points, yielding 8 ensembles for each TDS event. We assume that the two orthogonal antennas are measuring the same wave field and allow a phase shift between the two

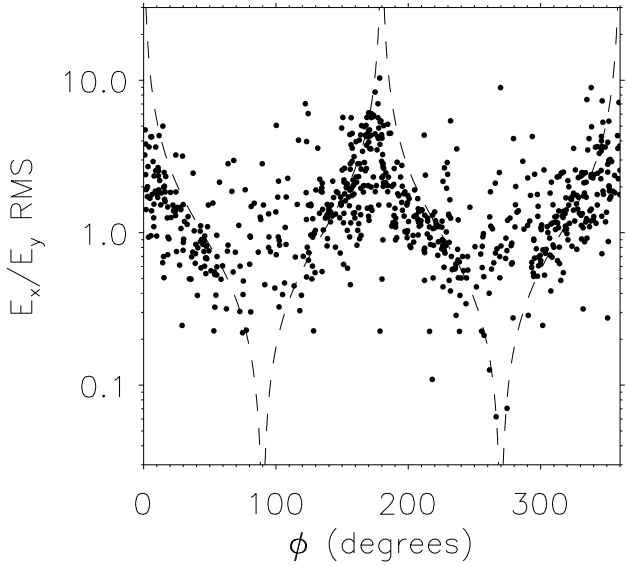


Figure 1. The ratio of RMS electric field on the X to Y antennas as a function of the angle between the X dipole and the IMF in the spin plane (antenna azimuth).

components; if one then assumes that the Fourier transform consists of a wave field superposed on a decoherent noise background N , one can write $\tilde{S}_x(\omega) = \tilde{N}_x(\omega) + E_x(\omega) e^{-i\omega t}$ and $\tilde{S}_y(\omega) = \tilde{N}_y(\omega) + E_y(\omega) e^{-i(\omega t + \delta(\omega))}$ for the Y component. Then, the cross spectrum defined above becomes

$$\tilde{C}(\omega) = \frac{1}{\sqrt{(1 + |\tilde{N}_x(\omega)|^2)(1 + |\tilde{N}_y(\omega)|^2)}} e^{i\delta(\omega)} \quad (2)$$

after carrying through the ensemble averages. So, the phase of the cross spectrum gives the phase shift between the two components and the magnitude gives the coherence between the two signals. This calculation assumes that the waves are roughly planar, which seems reasonable given their small bandwidth.

Figure 2 shows the phase δ at the peak frequency against the antenna azimuth ϕ . The peak frequency is identified from the power spectrum and we use the phase and coherence at this frequency. The coherence between the signals is uniformly large (≈ 1) and the calculation is robust to reasonable changes in ensemble size. Waves are only included when the peak frequency lies in the range $f \in (0.9, 1.3)f_{pe}$, to exclude beam modes, ion acoustic waves, and second harmonic radio emission.

As seen in Figure 2, the phase shift at the carrier frequency is nonzero and is a strong function of the angle between the antennas and the IMF; in particular the X-Y phase shift approaches ± 90 degrees when the X antenna is field aligned and recedes toward zero otherwise. Qualitatively, the trend in Figure 2 suggests that the phase is proportional to $-1/\tan\phi$ and evokes the notion of a resonance cone. Figure 3 shows the phase δ plotted against α , the absolute angle between the X antenna and the IMF. Again, it can be seen that phase shift is generally large for the field aligned component and smaller as the antenna measures at larger angles.

Figure 4 shows the measured X and Y electric field sig-

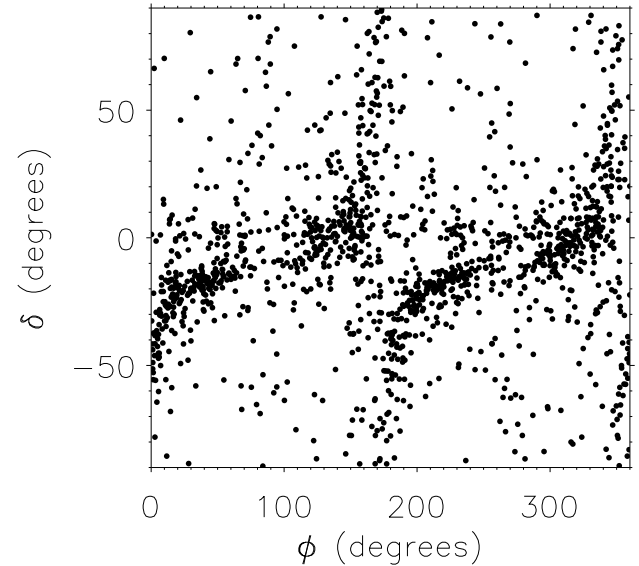


Figure 2. The average phase at peak frequency as function of antenna azimuth.

nals for a typical event with small average phase shift. In the lower panels, the running phase shift is plotted, as calculated from sliding 64 point ensembles and below that 128 point electric field hodograms. The hodograms are normalized to the maximum value in each component, so that a circularly polarized field would appear as a perfect circle. The phase is mostly constant and near zero, with a slight change near the minimum in the wavepacket. Figure 5 shows an event with a large average phase shift, in the same format. An obvious and interesting observation is that the shape of the wavepackets is different between the two antennas; this qualitative difference is related to the large average phase shift. It can also be seen that the largest changes in phase occur at nulls in the wavepacket. The hodogram for this

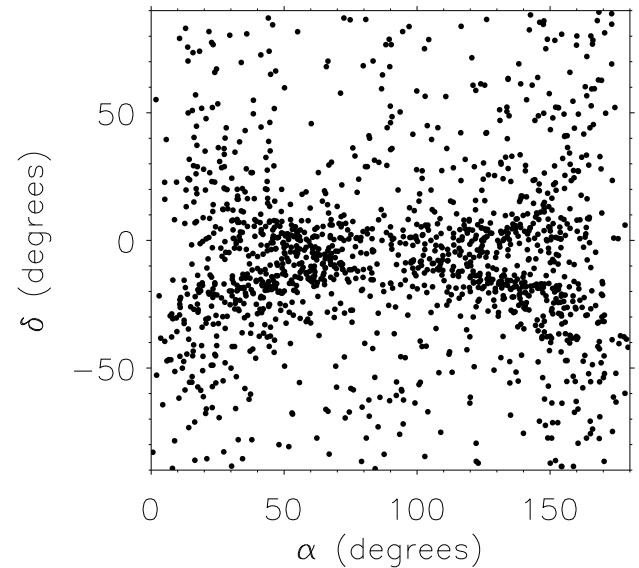


Figure 3. The average phase at peak frequency against the absolute antenna-IMF angle

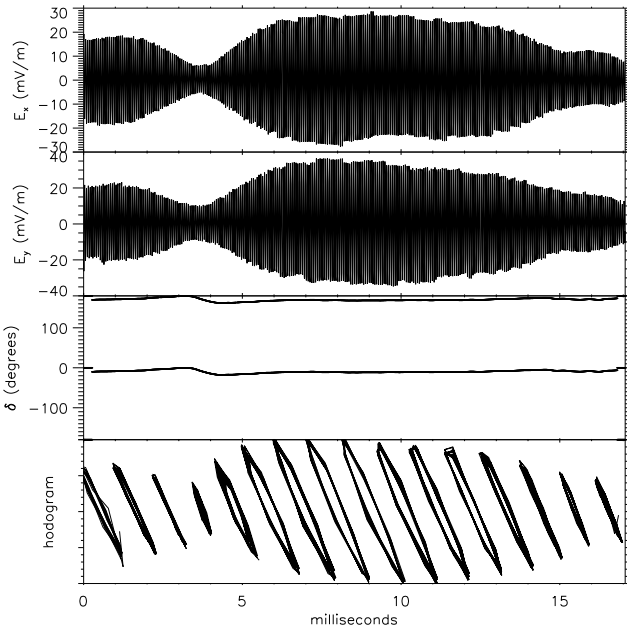


Figure 4. Electric field on the X and Y antennas (upper and second panel), the instantaneous phase shift (third panel), and 128 point hodograms (lower panel). This event has very small average phase and the waveform envelopes are very similar

event is quite stunning and shows very clearly the transverse nature of the wave, as well as a change in sign of the phase.

Interpretation

Our observations show that the waves previously identified as Langmuir waves, in the foreshock, have a significant transverse component consistent with long wavelength z -mode waves. Of course, the solar wind is a magnetized plasma and, as such, does not support the simple unmagnetized Langmuir mode. For large index of refraction $N^2 \approx k^2 c^2 / \omega_{pe}^2 \gg 1$, the z -mode is a longitudinally polarized, electrostatic wave with dispersion $\omega^2 = \omega_{pe}^2 + 3k^2 v_{th}^2 + \Omega_{ce}^2 \sin^2 \theta$ (θ is the propagation angle), nearly identical to the Langmuir wave for $\Omega_{ce}/\omega_{pe} \ll 1$. For $N^2 \ll 1$ however, the z -mode becomes a transverse, left-handed electromagnetic wave and crosses the o -mode branch for $\theta = 0$, with a cutoff at $\omega = -\Omega_{ce}/2 + \sqrt{\omega_{pe}^2 + \Omega_{ce}^2}/4$.

Krauss-Varban [1989] showed that the growth rate and unstable wavenumber of the beam-driven z -mode in the solar wind are virtually identical to those of the unmagnetized Langmuir mode. Furthermore, in the WKB approximation, the change in refractive index due to small density fluctuations in the solar wind is an important factor. Krauss-Varban [1989] showed that density fluctuations $\delta n/n$ of one percent can easily move the z -mode to very long wavelengths. Indeed, it can be seen by considering the index of refraction of simple Langmuir waves $N^2 \approx k^2 c^2 / \omega_{pe}^2 = c^2 / 3v_{th}^2 (\omega^2 / \omega_{pe}^2 - 1)$. In the presence of small density fluctuations, with scales larger than the typical foreshock resonant Langmuir wavelength (≈ 400 m), the WKB approximation obtains and the wave frequency can be considered constant, with k and E varying to sat-

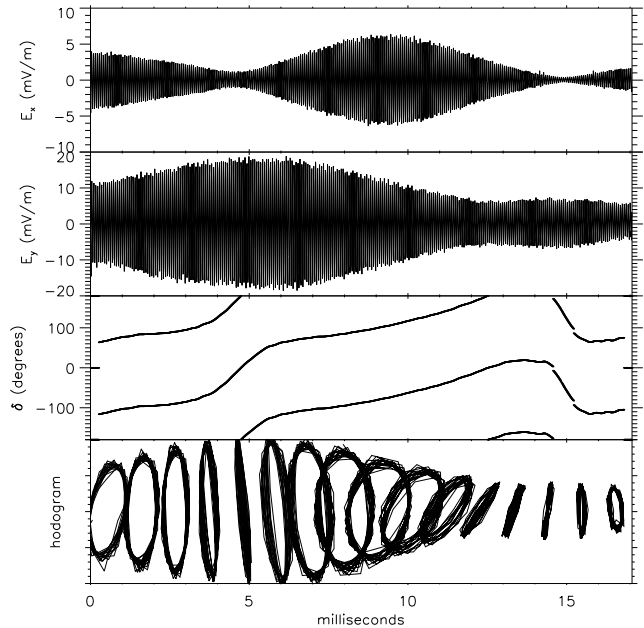


Figure 5. Electric field on the X and Y antennas (upper and second panel), the instantaneous phase shift (third panel), and 128 point hodograms (lower panel). When the antennas are more field aligned, the electric field wavepackets are dissimilar and the average phase shift is large. The instantaneous phase varies quickly near nulls in the wavepacket and the polarization, in this frame, may change sign.

isfy the dispersion relation locally. In this approximation, $\delta N^2 \approx -(c^2/3v_{th}^2)(\delta n/n) \approx -7500 \delta n/n$ for typical solar wind parameters; for very small levels of density fluctuations, the change in refractive index is large. For beam resonant upstream waves with $N_0^2 \approx 900$, the fluctuations in N^2 take it quickly to zero or the Landau damping scale $N_d^2 \approx 7500$.

The effect of density fluctuations on wave growth and damping has been considered by various authors [e. g. Muschietti *et al.*, 1985; Cairns, 1987] and any review is beyond the intention of this letter. However, most of this work has been done in the unmagnetized plasma approximation.

The prospect of linear mode conversion in such density fluctuations is interesting. When the propagation angle θ is small, the z -mode and o -mode branches approach one another for $N^2 \sim \Omega_{ce}/(\Omega_{ce} + \omega_{pe}) \ll 1$; thus for waves initially resonant with a nearly field aligned beam, the z -mode may convert by tunneling to freely propagating o -mode in the fluctuations, although the efficiency of this process depends on the density fluctuation spectrum. Emission near f_{pe} is sometimes observed near large density gradients in the solar wind [e. g. Burgess *et al.*, 1987] and this process may be ubiquitous in the solar wind, perhaps in fundamental type III burst emission as well as the foreshock.

The long wavelength, transverse nature of the waves has implications for wave saturation mechanisms as well. Since density fluctuations may take the waves out of resonance with the beam quickly, the maximum amplitude may depend strongly on, and be limited by, the solar wind density fluctuation spectrum. The wave amplitude probability distribution in the foreshock has been shown to have the form

$P(E) \propto 1/E^2$ [Bale et al., 1997] and wave growth is normally distributed on smaller scales [Cairns and Robinson, 1997]. Small k nonlinear saturation mechanisms, namely the electrostatic modulational instability, have little relevance as the waves are effectively transverse in this regime.

The electric field measurements presented here are typical, large amplitude (≥ 0.1 mV/m) foreshock waves; while smaller amplitude waves may show somewhat different properties, these results seem to hold generally near the electron foreshock-solar wind boundary.

Acknowledgments. SDB would like to thank I. H. Cairns, L. Muschietti, and A. J. Willes for useful comments. We thank the MFI team at GSFC for providing the spin resolution magnetic field data.

References

- Bougeret, J.-L., et al., WAVES: The radio and plasma wave investigation on the Wind spacecraft, *Space Sci. Rev.*, **71**, 231, 1995.
- Bale, S. D., D. Burgess, P. J. Kellogg, K. Goetz, and S. J. Monson, On the amplitude of intense Langmuir waves in the terrestrial electron foreshock, *J. Geophys. Res.*, **102**, 11,281, 1997.
- Burgess, D., C. C. Harvey, J.-L. Steinberg, and C. Lacombe, Simultaneous observation of fundamental and second harmonic radio emission from the terrestrial foreshock, *Nature*, **330**, 732, 1987.
- Cairns, I. H., A theory for the Langmuir waves in the electron foreshock, *J. Geophys. Res.*, **92**, 2329, 1987.
- Cairns, I. H., and P. A. Robinson, First test of stochastic growth theory for Langmuir waves in Earth's foreshock, *Geophys. Res. Lett.*, **24**, 369, 1997.
- Filbert, P. C., and P. J. Kellogg, Electrostatic noise at the plasma frequency beyond the Earth's bow shock, *J. Geophys. Res.*, **84**, 1369, 1979.
- Krauss-Varban, D., Beam instability of the z mode in the solar wind, *J. Geophys. Res.*, **94**, 3527, 1989.
- Muschietti, L., M. V. Goldman, and D. Newman, Quenching of the beam-plasma instability by large-scale density fluctuations in 3 dimensions, *Solar Phys.*, **96**, 181, 1985.
-
- S. D. Bale, Space Sciences Laboratory, University of California, Berkeley, CA, 94720-7450 USA (email: bale@ssl.berkeley.edu)
- K. Goetz, P. J. Kellogg, and S. J. Monson, School of Physics and Astronomy, University of Minnesota, Minneapolis, MN, 55455.

(Received August 19, 1997; revised October 2, 1997; accepted November 24, 1997.)